Spider silk reinforced by graphene or carbon nanotubes

Spider silk reinforced by graphene or carbon nanotubes

Emiliano Lepore[1], Federico Bosia[2], Francesco Bonaccorso[3,4], Matteo Bruna[3], Simone Taioli[5,6], Giovanni Garberoglio[5], Andrea. C. Ferrari[3], Nicola Maria Pugno[1,7,8*]

[1] Laboratory of Bio-inspired & Graphene Nanomechanics, Department of Civil, Environmental and Mechanical Engineering, University of Trento, Via Mesiano 77, 38123 Trento, Italy.
[2] Department of Physics and "Nanostructured Interfaces and Surfaces" Centre, Università di Torino, Via P. Giuria 1, 10125, Torino, Italy.
[3] Cambridge Graphene Centre, University of Cambridge, 9 JJ Thomson Avenue, Cambridge, CB3 0FA, UK
[4] Istituto Italiano di Tecnologia, Graphene Labs, Via Morego 30, 16163 Genova, Italy.
[5] European Centre for Theoretical Studies in Nuclear Physics and Related Areas, Bruno Kessler Foundation & Trento Institute for Fundamental Physics and Applications, Trento, Italy.
[6] Faculty of Mathematics and Physics, Charles University, Prague, Czech Republic.
[7] School of Engineering and Materials Science, Queen Mary University, Mile End Road, London E1 4NS, UK.
[8] Ket Lab, Edoardo Amaldi Foundation, Italian Space Agency, Via del Politecnico snc, 00133 Rome, Italy.

[*]Corresponding author: nicola.pugno@unitn.it

Abstract

Spider silk has promising mechanical properties, since it conjugates high strength (~1.5GPa) and toughness (~150J/g). Here, we report the production of silk incorporating graphene and carbon nanotubes by spider spinning, after feeding spiders with the corresponding aqueous dispersions. We observe an increment of the mechanical properties with respect to the pristine silk, up to a fracture strength ~5.4 GPa and a toughness modulus ~1570 J/g, the highest reported to date for any fibre. This approach could be extended to other biological systems and lead to a new class of artificially modified biological, or "bionic", materials.

Introduction

Silkworm silks have been widely used by mankind for millennia, but only recently their mechanical properties and structure have been studied in depth [1, 2]. An increasing number of studies also focuses on spider silk, due to its promising mechanical (~10 GPa Young's modulus, ~1.5 GPa strength [3, 4], ~ 100% ultimate strain [5]) and thermal properties (~400 W/m·K thermal conductivity [6]), combined with biocompatibility [7] and biodegradability [5, 7, 8]. This makes it potentially useful in practical applications such as wear-resistant lightweight clothing [9], bullet-proof vests [10], ropes [11], nets [12], bandages [13], surgical threads [14], artificial tendons or ligaments [15], and even biodegradable food wraps [16] or rust-free panels on vehicles [17]. For example in Ref. [18], researchers used individual spider silk fibres braided together to create sutures for flexor tendon repair. Enhanced Silk mechanical properties could further improve the fatigue strength and lifetime of these structures.

The production of silk is key to the spiders' evolutionary success and has been perfected over 400 million years [7]. It is generally described as a semi-crystalline [19], biocompatible [7], composite biopolymer [5], and comprises the amino acids alanine, glycine and serine, organized into semi-amorphous helical-elastic α-chains and β-pleated nanocrystals [20, 21]. From a mechanical point of view, it is considered amongst the best spun polymer fibres in terms of tensile strength [3, 4] and ultimate strain [5], and therefore toughness [11], even when compared with the best performing

synthetic fibres, such as Kevlar [22]. Silk spinning involves a number of biological, chemical and physical processes [23], leading to its superior mechanical properties.

The natural presence of biominerals in the protein matrix and hard tissues of insects [24], worms [25] and snails [26] enables high strength and hardness (>500MPa) of teeth [27, 28], jaws [28, 29], mandibles [30, 31]. Thus, the artificial incorporation of various nanomaterials in biological protein structures to obtain improved mechanical properties should be in principle possible. A number of groups introduced inorganic nanoparticles [32], semiconducting crystals [33] or carbon nanotubes (CNTs) [34] on the surface of spider silk fibres, achieving an enhancement of toughness [35], or novel properties, such as magnetism [32] or electrical conductivity [34]. This type of reinforcement or functionalization could further make silk potentially attractive for a wide range of applications, from garment textiles [9] to sensing devices [36], from medical applications, such as suture threads [14] or tissue regeneration materials [15], to defence applications such as flak jackets [10], currently limited by silk's large deformability [37-40].

Successful attempts to improve the mechanical properties of spider silk have been limited [36, 41]. This is due to the difficulty of developing an adequate spinning methodology, balancing extrusion, drawing, yield and purity [42]. Naturally-spun fibres, obtained by forcible spinning [43], harvesting [44] or extracting spidroin (i.e. the main protein in dragline silk [2]) from glands [45], have reduced mechanical characteristics with respect to naturally-spun ones, e.g. due to the CO_2 anaesthesia of spiders [46] and the consequent loss of active control of their silk spinning [47]. From a technological point of view, wet-spinning [48], electro-spinning [49], hand-drawing [43] or microfluidic approaches [50] have been investigated to produce an artificial silk at the laboratory scale, mechanically [36], structurally [41] or chemically [50] modified with respect to the natural one. However, a critical step is still needed to reach commercial-scale.

Here, we present a method for producing reinforced spider silk directly spun by spiders after their exposure to water dispersions of CNTs or graphene, as schematically shown in Fig. 1. This leads to improved mechanical properties, and a toughness modulus (defined as the area under the load-displacement curve, from the origin up to fracture [51, 52], per unit mass) surpassing synthetic polymeric high-performance fibres [53] and even the current toughest "knotted" fibres [54, 55].

Methods

Two types of CNTs are used in this study. The first is CoMoCAT [56] single-wall nanotubes (SWNT-1) . The second is electric arc discharge SWNT (P2) from Carbon solutions inc. (SWNT-2). CNT dispersions are prepared by adding 1 mg/10 ml weight-to-volume ratios of each CNT source to an aqueous solution of 2% w/v sodium deoxycholate (SDC, from Sigma-Aldrich Ltd.) in deionised water. This surfactant is not harmful for the spiders, as discussed in the S.I. De-bundling is obtained via ultrasonication using a Branson Ultrasonic Processor for 2 hours (450 kW at 20 kHz). The dispersions are ultracentrifuged using a TH-641 swinging bucket rotor in a Sorvall WX-100 at 200,000g for 2 hours at 18°C to remove bundles and other impurities, such as amorphous carbon and catalyst residuals [57]. The supernatant of the two dispersions after ultracentrifugation is collected using pipettes and used for the characterization. Graphite flakes are sourced from Sigma Aldrich Ltd. 100 mg are dispersed in 10ml water with 2% v/w SDC. The dispersion is then ultrasonicated for 10 hours and subsequently ultracentrifuged, exploiting sedimentation-based separation (SBS) [58] using a TH-641 swinging bucket rotor in a Sorvall WX-100 ultracentrifuge at 5000 rpm for 30 mins. After ultracentrifugation, the supernatant is extracted by pipetting. The concentration of graphitic flakes (i.e., ~0.03mg/ml) is determined from the optical absorption coefficient at 660nm [59] A full optical and spectroscopic characterization of the samples is presented in Supplementary Information (S.I.), which indicate the samples being composed by ~60% of single- (SLG) and ~40% few-layer (FLG) graphene flakes [60].

21 spiders of three different species were selected (*Pholcidae Holocnemus, Pholcidae Pholcus* and *Theridiidae Steatoda*) as described in the S.I. The spiders were exposed to the aqueous dispersions

by spraying them in a corner of the box they were contained in, avoiding intentional direct spraying on the animals. The dragline silk was collected from 2 to 12 days later, in order to allow sufficient time for ingestion of the aqueous dispersions and the production of silk. 29% of the spiders died before the first silk collection, and a further 24% after 12 days, during which starvation could have come into play. The silk fibres consisted of multiple threads of approximately circular cross-section. The average diameter of the single threads was determined for each sample through Field Emission Scanning Electron Microscopy (see S.I.), at two different cross-sections along their length. The number of threads in each fibre was also counted. The presence of CNTs and graphene was monitored by Raman spectroscopy.

Nano-tensile tests were performed under controlled conditions as described in the S.I. Samples are prepared by fixing silk fibre ends to "C" shaped cardboard holders (then cut after mounting in the sample holder, Fig. 1b), and subjected to traction up to failure in an Agilent T150 nanotensile system at a constant strain rate of 0.1 %/s, consistently with previous studies on spider silk mechanics [4, 61-63]. The stress σ, strain ε, and Young's modulus E, are calculated as $\sigma = F/A_0$, $\varepsilon = \Delta l/l_0$, $E = \mathrm{d}\sigma/\mathrm{d}\varepsilon\big|_0$, where F is the force measured by the adopted nanotensile system (see S.I. for details), A_0 is the cross-section area of the fibre, l_0 its initial length, and Δl the change in fibre length measured during the test. The area underlying the stress-strain curve corresponds to the energy per unit volume required to break the fibre, i.e. the so-called toughness modulus T, also alternatively given in energy per unit mass, as derived by dividing the energy per unit volume by the density of the material: $T = \frac{1}{\rho}\int \sigma d\varepsilon$ [64].

Results

The diameter of the cross-sectional area of the silk fibres is found to be typically between ~5 and ~10μm, obtained by multiplying the mean value of the measured cross-sectional area of the threads by their total number. The resulting diameters and number of threads for each fibre are reported in Tables 1, 2 for the reference spider silk (RS) and that collected from spiders exposed to dispersions of graphene (GS) and SWNTs (CNTS).

Fig. 2 shows an optical image of a suspended fibre (Fig. 2a) and compares the Raman spectra of RS with that of GS (Fig. 2b) and CNTS (Fig. 2 c,d). The RS Raman spectrum comprises several peaks in the 1000-1800 cm^{-1} and 2700-3500 cm^{-1} regions. The peaks at ~1088 and 1160cm^{-1} are characteristic of the n(C-C) skeletal band of polypeptide chains [65, 66]. Two intense bands are also seen at ~1230 cm^{-1}, characteristic of amide III groups in π-sheets structured proteins [67, 68] and at ~1444cm^{-1} assigned to CH_2 bending modes, both bands typically found in the Raman spectrum of spider silk [69]. The peaks at 1615cm^{-1} and 1665cm^{-1} are assigned to n(CO) amide I bands characteristic of the π-sheets configuration for the polypeptide backbone [67, 69]. The Raman peaks in the region 2700-3500 cm^{-1} are typical of C-H and N-H vibrations [68].

Raman spectra from GS and CNTS samples are shown in Fig. 3. The spectra are normalized with respect to the C-H band at ~2934cm^{-1}, the most intense in RS. The normalized RS spectrum is then subtracted from the GS and CNTS ones. Figs. 3a,b show that the spectrum of the graphene flakes in the dispersion is compatible with that of GS. At both 514 and 633nm, the D to G and 2D to G intensity ratios, I(D)/I(G) and I(2D)/I(G), as well as the positions of the G and 2D peaks, Pos(G) and Pos(2D), are very similar. The comparison indicates that graphene detected in GS has a similar level of disorder [70-73] as the original material. The same holds for the case of CNTS. Figs 2c-f show that the spectra of the original SWNTs and those measured on CNTS are similar, indicating a negligible change in the structural properties.

A summary of the mechanical properties of RS, GS and CNTS are reported in Tables 1-2, and typical stress-strain curves of the silk fibres are presented in Fig. 1c and in the S.I. Scatter in the data is considerable, mainly due to the variability in the properties of the collected silk samples, deriving from spiders of different species and ages (see S.I.), but also from factors such as the sensitivity of

silk density from humidity [74]. However, fibre slippage in the loading frame can be excluded, since this would also have been be noticeable in the measured stress-strain curves, given the high-sensitivity (50 nN load resolution and 0.1 nm displacement resolution) of the nanotensile testing system. Ultimate strain values display smaller scatter, since they are not dependent on parameters such as fibre cross-sectional area. In the case of the reinforced silk samples, the scatter is increased due to the strongly varying reinforcement concentrations, since there is no control on the nanoparticle uptake mechanism at this stage. Apart from this, there is an intrinsic variability of mechanical properties of different samples of the same silk, in line with previous studies [62, 75-77].

To avoid these problems, we focus on the variation in mechanical properties of the silk fibres from individual spider specimens before and after exposure. The average and maximum variations are shown in Fig. 4. Fracture strength, Young's modulus and toughness increase on average between 80 and 220 % in CNTS and between 15% and 60% for GS. The highest fracture strength and Young's modulus increments are +731% (3.9 GPa) and +1183% (37.9 GPa) for CNTS, with an increment ~+663% in toughness (2.1 GPa). This corresponds to 1567 J/g, calculated using an average silk density value of 1.34 g/cm^3 [64], neglecting changes due to humidity variations or the presence of CNTs or graphene, as discussed in the S.I., with a 41% decrement of ultimate strain (0.6 mm/mm). This should be compared to the toughest silk fibres found to date, having a toughness ~520 MJ/m^3 [62], and a strength ~1.65 GPa [62]. The combination of increment in toughness and decrement in ultimate strain is peculiar and fundamental in applications such as parachutes or bullet-proof vests, where high performance textiles are required to stop bullets in millimetres [78]. The second highest increments ~+350% (2.0 GPa) in fracture strength and +330% (19.3 GPa) in Young's modulus are found for SWNT-2-CNTS, corresponding to an increment ~+204% in toughness (0.4 GPa), with a decrement ~36% in ultimate strain (0.3 mm/mm). A smaller, but still significant, increment is also observed for some of the fibres containing GS, with +151% (1.2 GPa) in fracture strength and +142% (13.0 GPa) in Young's modulus, corresponding to an increment of both toughness and ultimate strain of +250% (0.3 GPa) and +166% (0.4 mm/mm), respectively.

We note that Ref. [79] reported a similar approach to that described here, based on the initial posting of the present manuscript [80], cited as Ref. [19] in [79] and applied it to silkworm silk. This demonstrates that our approach is reproducible in other biological systems. However, Ref. [79] achieved far inferior mechanical properties to those reported here. Indeed, in the best case we get here a strength ~ 5.4 GPa and toughness modulus ~1567 J/g, whilst Ref. [79] achieves maximum values ~0.6 GPa and ~400 J/g, respectively. This is mainly due to lower mechanical properties of silkworm silk with respect to spider silk [1-4].

Discussion

Figure 5 shows a comparison between the strength and toughness of various natural and artificial materials displaying notable mechanical properties. The best fibre obtained in this study displays higher strength than high-performance polymeric fibres like Zylon or Endumax [53, 54], or SWNT/carbon-reinforced polymeric fibres [81-83], and is surpassed only by T1000® Carbon fibres [84] or goethite nanofibers found in limpet teeth [27]. At the same time, its toughness is significantly higher than the toughest spider silks found in nature [62, 76] or high-toughness SWNT/PVA fibres [81]. Indeed, it exceeds the previous largest recorded toughness value for synthetic polymer fibres or carbon nanotube microfibres with integrated knots as energy dissipators [54].

Molecular Dynamics simulations reported in the S.I. show that CNTs have the strongest interaction with the MASP1 spider silk fibers, in the amorphous region where they affect the structure of the bundle. The measured strength and stiffness data can be compared to analytical predictions for the reinforcing effect of graphene or CNTs on silk using the direct and inverse rule of mixtures [85] and simulations using the Hierarchical Fibre Bundle Model [86] (see S.I.). These can be used to estimate the concentration of reinforcements by fitting the corresponding experimental strength

values, giving equivalent volume fractions in GS and CNTS between 1% (spider 15) and 15% (spider 7), with an average ~7%.

On average, graphene appears to be a less effective reinforcement than CNTs (Fig. 4c). This could be due to a reduced concentration, due to the shape of the flakes. Also, the lateral characteristic dimensions of our flakes (~200-300 nm), two orders of magnitude larger than the characteristic CNT diameter, could give rise to less efficient load transfer, since their longitudinal dimension could be smaller than the critical length (of the order of microns and dependent on the interface properties) predicted by the shear lag theory for optimal load transfer [87]. Inefficient load transfer could also be due to the flakes crumpled configuration or a larger misalignment with respect to CNTs. Finding solutions for these problems could potentially enable GS with mechanical properties superior to CNTS, thanks to the two surfaces available for load transfer in flakes [87]. Tuning the constitutive law of the silk could also maximize the robustness of an entire structure [88]. The insertion could also be used to enhance the toughness.

Conclusions

Spiders placed in an environment with water solutions containing nanotubes or graphene produce dragline silk with enhanced mechanical properties, in the best case realizing the highest fibre toughness to date, combined with a strength comparable to that of the strongest carbon fibres or of limpet teeth. This proof-of-concept experiment paves the way to exploiting the naturally efficient spider spinning process to produce reinforced silk fibres, thus further improving one of the most promising silk materials, as compared to synthetic recombinant silks. This procedure of natural integration of reinforcements in biological structural materials could also be applied to other animals and plants, leading to a new class of "bionicomposites" for innovative applications.

Acknowledgments

We acknowledge "Nanofacility Piemonte" at the INRIM Institute for the FESEM, a Newton International Fellowship, EPSRC grants EP/K01711X/1, EP/K017144/1, ERC grant SILKENE, Hetero2D, HiGRAPHINK, FET Proactive NEUROFIBRES and the EU Graphene Flagship. This paper is dedicated to the memory of prof. Franco Montevecchi.

References

[1] Shao Z Z and Vollrath F 2002 Materials: Surprising strength of silkworm silk *Nature* **418** 741-
[2] Atkins E 2003 Silk's secrets *Nature* **424** 1010-
[3] Agnarsson I, Boutry C and Blackledge T A 2008 Spider silk aging: Initial improvement in a high performance material followed by slow degradation *J Exp Zool Part A* **309A** 494-504
[4] Swanson B O, Blackledge T A, Beltran J and Hayashi C Y 2006 Variation in the material properties of spider dragline silk across species *Appl Phys a-Mater* **82** 213-8
[5] Vollrath F, Porter D and Holland C 2013 The science of silks *Mrs Bull* **38** 73-80
[6] Huang X P, Liu G Q and Wang X W 2012 New Secrets of Spider Silk: Exceptionally High Thermal Conductivity and Its Abnormal Change under Stretching *Adv Mater* **24** 1482-6
[7] Foelix R F 2011 *Biology of spiders* (Oxford ; New York: Oxford University Press)
[8] Eisoldt L, Smith A and Scheibel T 2011 Decoding the secrets of spider silk *Mater Today* **14** 80-6
[9] Byrom D 1991 *Biomaterials: Novel Materials from Biological Sources*: Palgrave Macmillan UK)
[10] Laible R 2012 *Ballistic Materials and Penetration Mechanics*: Elsevier Science)
[11] Kubik S 2002 High-performance fibers from spider silk *Angew Chem Int Edit* **41** 2721-+
[12] Scott A 2014 Spider Silk Poised For Commercial Entry *Chem Eng News* **92** 24-7
[13] Harvey D, Bardelang P, Goodacre S L, Cockayne A and Thomas N R 2017 Antibiotic Spider Silk: Site-Specific Functionalization of Recombinant Spider Silk Using "Click" Chemistry *Adv Mater* **29**

[14] Kuhbier J W, Reimers K, Kasper C, Allmeling C, Hillmer A, Menger B, Vogt P M and Radtke C 2011 First investigation of spider silk as a braided microsurgical suture *Journal of Biomedical Materials Research Part B: Applied Biomaterials* **97B** 381-7
[15] Allmeling C, Jokuszies A, Reimers K, Kall S, Choi C Y, Brandes G, Kasper C, Scheper T, Guggenheim M and Vogt P M 2008 Spider silk fibres in artificial nerve constructs promote peripheral nerve regeneration *Cell Proliferation* **41** 408-20
[16] Marelli B, Brenckle M A, Kaplan D L and Omenetto F G 2016 Silk Fibroin as Edible Coating for Perishable Food Preservation *Scientific Reports* **6**
[17] Babu K M 2013 *Silk : Processing, Properties and Applications* (Oxford, Cambridge, Philadelphia, New Delhi: Woodhead Publishing Limited LaVergne)
[18] Hennecke K, Redeker J, Kuhbier J W, Strauss S, Allmeling C, Kasper C, Reimers K and Vogt P M 2013 Bundles of Spider Silk, Braided into Sutures, Resist Basic Cyclic Tests: Potential Use for Flexor Tendon Repair *Plos One* **8** e61100
[19] Keten S and Buehler M J 2010 Nanostructure and molecular mechanics of spider dragline silk protein assemblies *J R Soc Interface* **7** 1709-21
[20] Silva L P and Rech E L 2013 Unravelling the biodiversity of nanoscale signatures of spider silk fibres *Nat Commun* **4**
[21] Porter D and Vollrath F 2009 Silk as a Biomimetic Ideal for Structural Polymers *Adv Mater* **21** 487-92
[22] Heim M, Keerl D and Scheibel T 2009 Spider Silk: From Soluble Protein to Extraordinary Fiber *Angew Chem Int Edit* **48** 3584-96
[23] Vollrath F, Madsen B and Shao Z Z 2001 The effect of spinning conditions on the mechanics of a spider's dragline silk *P Roy Soc B-Biol Sci* **268** 2339-46
[24] George A and Ravindran S 2010 Protein templates in hard tissue engineering *Nano Today* **5** 254-66
[25] Lichtenegger H C, Schoberl T, Bartl M H, Waite H and Stucky G D 2002 High abrasion resistance with sparse mineralization: Copper biomineral in worm jaws *Science* **298** 389-92
[26] Politi Y, Metzler R A, Abrecht M, Gilbert B, Wilt F H, Sagi I, Addadi L, Weiner S and Gilbert P U P A 2008 Transformation mechanism of amorphous calcium carbonate into calcite in the sea urchin larval spicule *Proceedings of the National Academy of Sciences* **105** 17362-6
[27] Barber A H, Lu D and Pugno N M 2015 Extreme strength observed in limpet teeth *J R Soc Interface* **12**
[28] Broomell C C, Zok F W and Waite J H 2008 Role of transition metals in sclerotization of biological tissue *Acta Biomaterialia* **4** 2045-51
[29] Broomell C C, Mattoni M A, Zok F W and Waite J H 2006 Critical role of zinc in hardening of Nereis jaws *Journal of Experimental Biology* **209** 3219-25
[30] Cribb B W, Stewart A, Huang H, Truss R, Noller B, Rasch R and Zalucki M P 2007 Insect mandibles—comparative mechanical properties and links with metal incorporation *Naturwissenschaften* **95** 17-23
[31] Edwards A J, Fawke J D, McClements J G, Smith S A and Wyeth P 1993 Correlation of zinc distribution and enhanced hardness in the mandibular cuticle of the leaf-cutting ant Atta sexdens rubropilosa *Cell Biology International* **17** 697-8
[32] Mayes E L, Vollrath F and Mann S 1998 Fabrication of magnetic spider silk and other silk-fiber composites using inorganic nanoparticles *Adv Mater* **10** 801-5
[33] Chu M Q and Sun Y 2007 Self-assembly method for the preparation of near-infrared fluorescent spider silk coated with CdTe nanocrystals *Smart Mater Struct* **16** 2453-6
[34] Steven E, Saleh W R, Lebedev V, Acquah S F A, Laukhin V, Alamo R G and Brooks J S 2013 Carbon nanotubes on a spider silk scaffold *Nat Commun* **4**
[35] Lee S-M, Pippel E, Gösele U, Dresbach C, Qin Y, Chandran C V, Bräuniger T, Hause G and Knez M 2009 Greatly Increased Toughness of Infiltrated Spider Silk *Science* **324** 488-92
[36] Steven E, Saleh W R, Lebedev V, Acquah S F A, Laukhin V, Alamo R G and Brooks J S 2013 Carbon nanotubes on a spider silk scaffold *Nature Communications* **4** 2435
[37] Allmeling C, Jokuszies A, Reimers K, Kall S and Vogt P M 2006 Use of spider silk fibres as an innovative material in a biocompatible artificial nerve conduit *J Cell Mol Med* **10** 770-7

[38] Dal Pra I, Chiarini A, Boschi A, Freddi G and Armato U 2006 Novel dermo-epidermal equivalents on silk ribroin-based formic acid-crosslinked three-dimensional nonwoven devices with prospective applications in human tissue engineering/regeneration/repair *Int J Mol Med* **18** 241-7
[39] Agnarsson I, Dhinojwala A, Sahni V and Blackledge T A 2009 Spider silk as a novel high performance biomimetic muscle driven by humidity *J Exp Biol* **212** 1989-93
[40] Dal Pra I, Freddi G, Minic J, Chiarini A and Armato U 2005 De novo engineering of reticular connective tissue in vivo by silk fibroin nonwoven materials *Biomaterials* **26** 1987-99
[41] Brown C P, Rosei F, Traversa E and Licoccia S 2011 Spider silk as a load bearing biomaterial: tailoring mechanical properties via structural modifications *Nanoscale* **3** 870-6
[42] Hardy J G, Romer L M and Scheibel T R 2008 Polymeric materials based on silk proteins *Polymer* **49** 4309-27
[43] Pérez-Rigueiro J, Elices M, Plaza G, Real J I and Guinea G V 2005 The effect of spinning forces on spider silk properties *J Exp Biol* **208** 2633-9
[44] Lewis R 1996 Unraveling the weave of spider silk: One of nature's wondrous chemical structures is being dissected so that it can be used in human inventions *BioScience* **46** 636-8
[45] Kenney J M, Knight D, Wise M J and Vollrath F 2002 Amyloidogenic nature of spider silk *European Journal of Biochemistry* **269** 4159-63
[46] Guinea G V, Elices M, Real J I, Gutierrez S and Perez-Rigueiro J 2005 Reproducibility of the tensile properties of spider (Argiope trifasciata) silk obtained by forced silking *Journal of Experimental Zoology Part a-Comparative Experimental Biology* **303A** 37-44
[47] Blackledge T A, Swindeman J E and Hayashi C Y 2005 Quasistatic and continuous dynamic characterization of the mechanical properties of silk from the cobweb of the black widow spider Latrodectus hesperus *Journal of Experimental Biology* **208** 1937-49
[48] Liu Y, Shao Z and Vollrath F 2005 Extended wet-spinning can modify spider silk properties *Chemical Communications* 2489-91
[49] Oh H J, Pant H R, Kang Y S, Jeon K S, Pant B, Kim C S and Kim H Y 2012 Synthesis and characterization of spider-web-like electrospun mats of meta-aramid *Polymer International* **61** 1675-82
[50] Peng Q, Zhang Y, Lu L, Shao H, Qin K, Hu X and Xia X 2016 Recombinant spider silk from aqueous solutions via a bio-inspired microfluidic chip *Scientific Reports* **6** 36473
[51] De Silva C W 2014 *Mechanics of materials* (Boca Raton: CRC Press)
[52] Rao D S 2002 *Introduction to Strength of Materials*: Universities Press)
[53] Bhat G 2017 *Structure and Properties of High-Performance Fibers,* (Oxford: Woodhead Publishing)
[54] Bosia F, Lepore E, Alvarez N T, Miller P, Shanov V and Pugno N M 2016 Knotted synthetic polymer or carbon nanotube microfibres with enhanced toughness, up to 1400 J/g *Carbon* **102** 116-25
[55] Pantano M F, Berardo A and Pugno N M 2016 Tightening slip knots in raw and degummed silk to increase toughness without losing strength *Scientific Reports* **6**
[56] www.sigmaaldrich.com/materials-science/nanomaterials/comocat-carbon-nanotubes.html.
[57] Bonaccorso F, Hasan T, Tan P H, Sciascia C, Privitera G, Di Marco G, Gucciardi P G and Ferrari A C 2010 Density Gradient Ultracentrifugation of Nanotubes: Interplay of Bundling and Surfactants Encapsulation *J Phys Chem C* **114** 17267-85
[58] Bonaccorso F, Lombardo A, Hasan T, Sun Z, Colombo L and Ferrari A C 2012 Production and processing of graphene and 2d crystals *Mater Today* **15** 564-89
[59] Torrisi F, Hasan T, Wu W P, Sun Z P, Lombardo A, Kulmala T S, Hsieh G W, Jung S J, Bonaccorso F, Paul P J, Chu D P and Ferrari A C 2012 Inkjet-Printed Graphene Electronics *Acs Nano* **6** 2992-3006
[60] Marago O M, Bonaccorso F, Saija R, Privitera G, Gucciardi P G, Iati M A, Calogero G, Jones P H, Borghese F, Denti P, Nicolosi V and Ferrari A C 2010 Brownian Motion of Graphene *Acs Nano* **4** 7515-23
[61] Lepore E, Marchioro A, Isaia M, Buehler M J and Pugno N M 2012 Evidence of the Most Stretchable Egg Sac Silk Stalk, of the European Spider of the Year Meta menardi *Plos One* **7**
[62] Agnarsson I, Kuntner M and Blackledge T A 2010 Bioprospecting Finds the Toughest Biological Material: Extraordinary Silk from a Giant Riverine Orb Spider *Plos One* **5** e11234
[63] Sahni V, Blackledge T A and Dhinojwala A 2010 Viscoelastic solids explain spider web stickiness *Nat Commun* **1** 19

[64] Pugno N M 2014 The "Egg of Columbus" for Making the World's Toughest Fibres *Plos One* **9**
[65] Colomban P, Dinh H M, Riand J, Prinsloo L C and Mauchamp B 2008 Nanomechanics of single silkworm and spider fibres: a Raman and micro-mechanical in situ study of the conformation change with stress *J Raman Spectrosc* **39** 1749-64
[66] Edwards H G M and Farwell D W 1995 Raman-Spectroscopic Studies of Silk *J Raman Spectrosc* **26** 901-9
[67] Williams A C, Barry B W and Edwards H G M 1994 Comparison of Fourier-Transform Raman-Spectra of Mammalian and Reptilian Skin *Analyst* **119** 563-6
[68] Socrates G 2004 *Infrared and Raman Characteristic Group Frequencies: Tables and Charts, 3rd Edition* (Chichester: Wiley)
[69] Shao Z, Vollrath F, Sirichaisit J and Young R J 1999 Analysis of spider silk in native and supercontracted states using Raman spectroscopy *Polymer* **40** 2493-500
[70] Ferrari A C and Basko D M 2013 Raman spectroscopy as a versatile tool for studying the properties of graphene *Nat Nano* **8** 235-46
[71] Bruna M, Ott A K, Ijäs M, Yoon D, Sassi U and Ferrari A C 2014 Doping Dependence of the Raman Spectrum of Defected Graphene *Acs Nano* **8** 7432-41
[72] Cançado L G, Jorio A, Ferreira E H M, Stavale F, Achete C A, Capaz R B, Moutinho M V O, Lombardo A, Kulmala T S and Ferrari A C 2011 Quantifying Defects in Graphene via Raman Spectroscopy at Different Excitation Energies *Nano Lett* **11** 3190-6
[73] Ferrari A C and Robertson J 2000 Interpretation of Raman spectra of disordered and amorphous carbon *Phys Rev B* **61** 14095-107
[74] Vehoff T, Glisovic A, Schollmeyer H, Zippelius A and Salditt T 2007 Mechanical properties of spider dragline silk: Humidity, hysteresis, and relaxation *Biophys J* **93** 4425-32
[75] Moore A M F and Tran K 1999 Material properties of cobweb silk from the black widow spider Latrodectus hesperus *Int J Biol Macromol* **24** 277-82
[76] Swanson B O, Blackledge T A, Summers A P and Hayashi C Y 2006 Spider dragline silk: correlated and mosaic evolution in high-performance biological materials *Evolution* **60** 2539-51
[77] Blackledge T A and Hayashi C Y 2006 Silken toolkits: biomechanics of silk fibers spun by the orb web spider Argiope argentata (Fabricius 1775) *Journal of Experimental Biology* **209** 2452-61
[78] Peleg K, Rivkind A and Aharonson-Daniel L 2006 Does Body Armor Protect from Firearm Injuries? *Journal of the American College of Surgeons* **202** 643-8
[79] Wang Q, Wang C Y, Zhang M C, Jian M Q and Zhang Y Y 2016 Feeding Single-Walled Carbon Nanotubes or Graphene to Silkworms for Reinforced Silk Fibers *Nano Lett* **16** 6695-700
[80] Lepore E, Bonaccorso, F., Bruna, M., Bosia, F., Taioli, S. Garberoglio, G., Ferrari, A. C., Pugno, N.M. 2015 Silk reinforced with graphene or carbon nanotubes spun by spiders *arXiv:1504.06751 [cond-mat.mtrl-sci]*
[81] Miaudet P, Badaire S, Maugey M, Derré A, Pichot V, Launois P, Poulin P and Zakri C 2005 Hot-Drawing of Single and Multiwall Carbon Nanotube Fibers for High Toughness and Alignment *Nano Lett* **5** 2212-5
[82] Dalton A B, Collins S, Munoz E, Razal J M, Ebron V H, Ferraris J P, Coleman J N, Kim B G and Baughman R H 2003 Super-tough carbon-nanotube fibres *Nature* **423** 703-
[83] Vilatela J J and Windle A H 2010 Yarn-Like Carbon Nanotube Fibers *Adv Mater* **22** 4959-+
[84] Liu J, Yue Z and Fong H 2009 Continuous Nanoscale Carbon Fibers with Superior Mechanical Strength *Small* **5** 536-42
[85] Askeland D R, Fulay P P and Wright W J 2011 *The science and engineering of materials* (Stamford, CT: Cengage Learning)
[86] Pugno N M, Bosia F and Abdalrahman T 2012 Hierarchical fiber bundle model to investigate the complex architectures of biological materials (vol 85, 011903, 2012) *Phys Rev E* **85**
[87] Pugno N M 2013 Towards the Artsutanov's dream of the space elevator: The ultimate design of a 35 GPa strong tether thanks to graphene *Acta Astronaut* **82** 221-4
[88] Cranford S W, Tarakanova A, Pugno N M and Buehler M J 2012 Nonlinear material behaviour of spider silk yields robust webs *Nature* **482** 72-U91

FIGURES

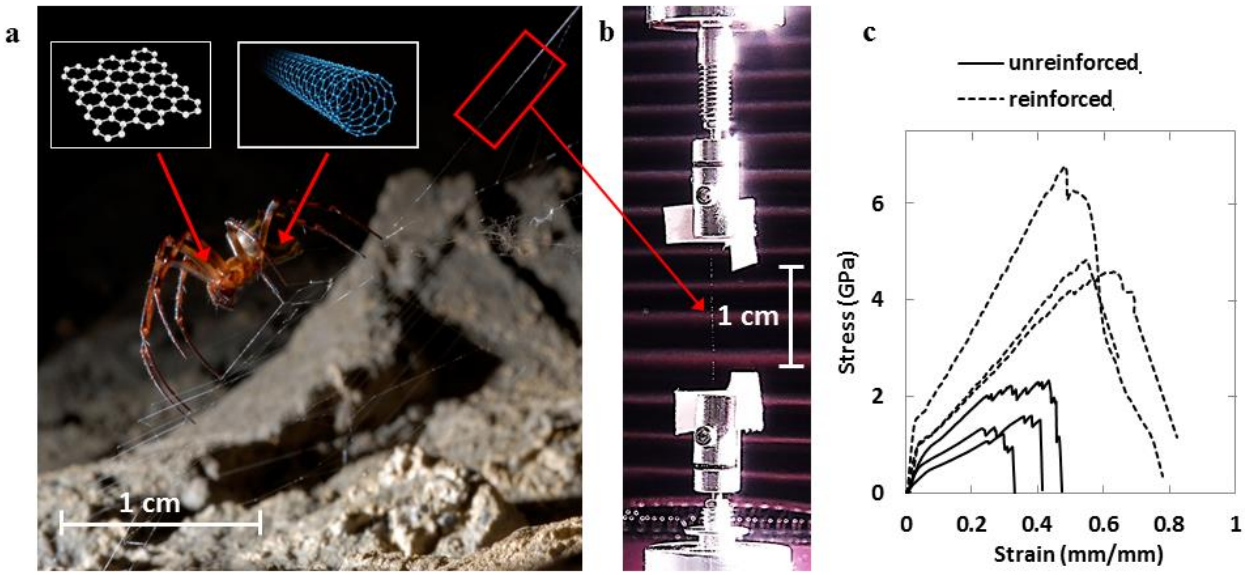

Figure 1: Schematic of the experimental procedure a) Spiders are fed solutions containing graphene or CNTs, b) the corresponding spun silk is collected and tested in a nanotensile system; c) stress-strain curves show improved mechanical properties.

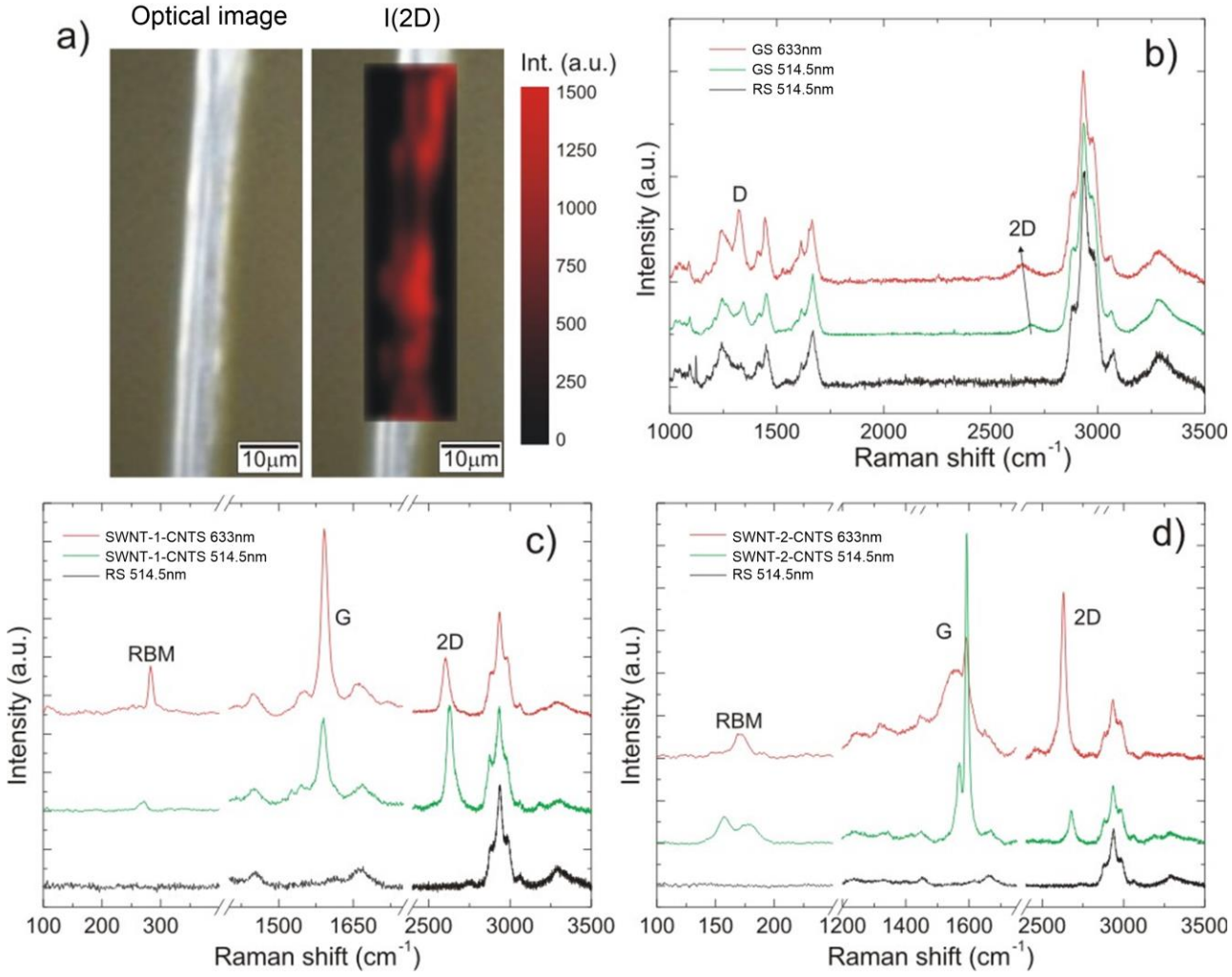

Figure 2: a) Optical picture of a spider silk fibre suspended by a mechanical support (left) and map of I(2D) overlapped to the optical picture of the spider silk spun by spiders after exposure to graphene (right). b) Raman spectra of RS (black line, at 514.5nm), GS at 514.5nm (green line) and 633nm (red line). Raman spectra of c) SWNT-1-CNTS d) SWNT-2-CNTS at 514.5nm (green line) and 633nm (red line) excitation wavelengths.

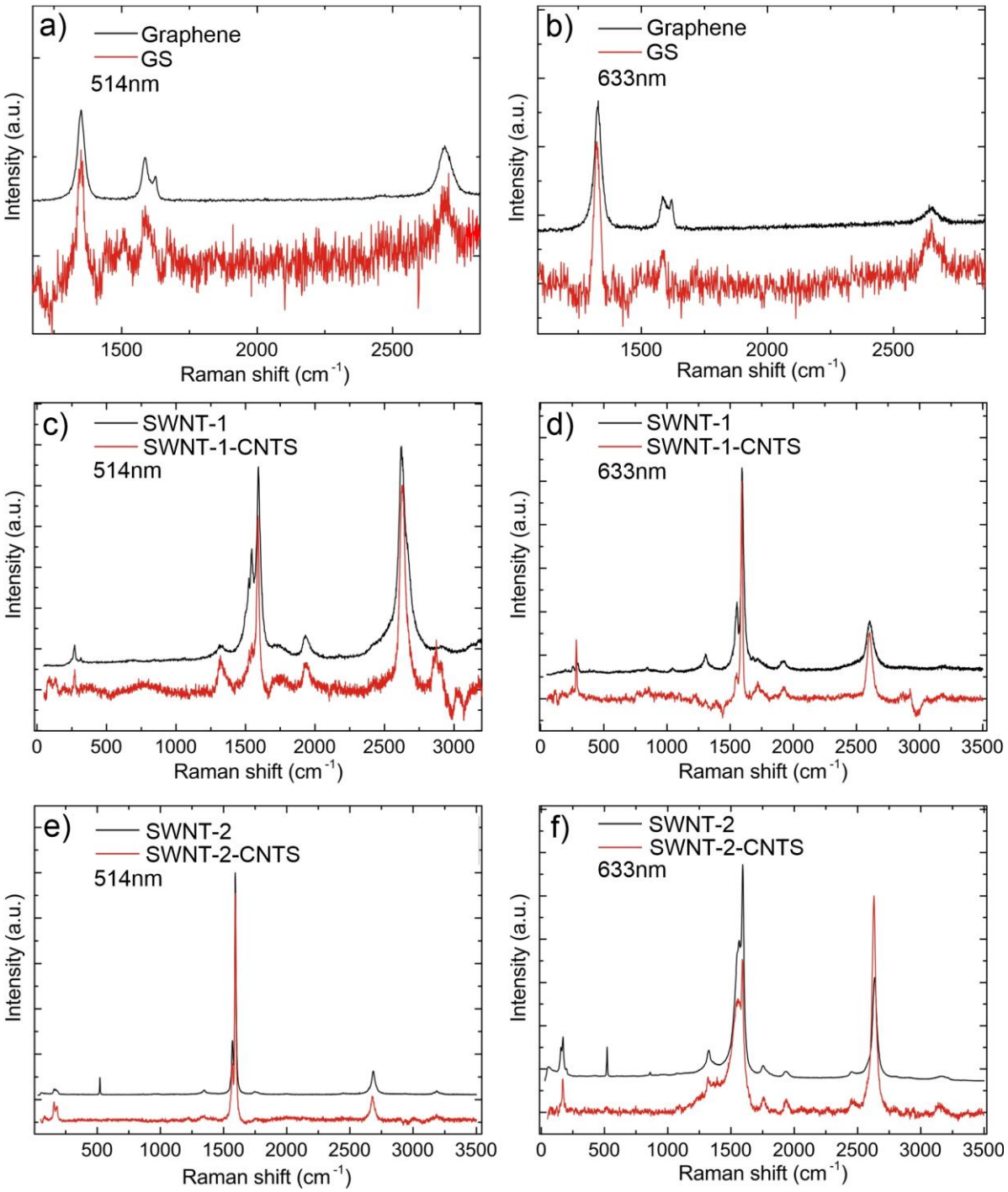

Figure 3: Raman spectra of graphene (black line) and GS (red line) at a) 514.5nm and b) 633nm. Raman spectra of c,d) SWNT-1, SWNT-2 and SWNT-1-CNTS and SWNT-2-CNTS at (c,e) 514.5nm and (d,f) 633nm excitation wavelengths.

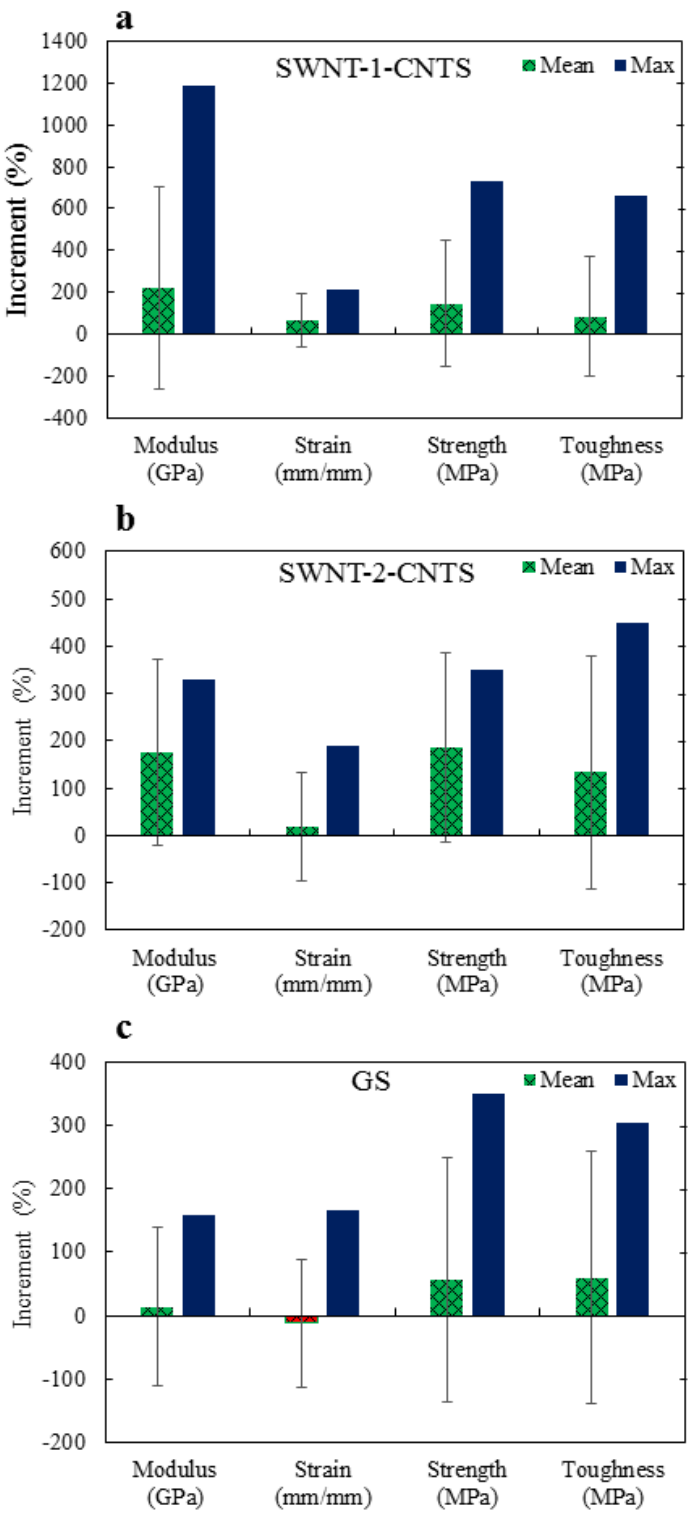

Figure 4: Percentage increment (green bars) or decrement (red bars) of the mechanical properties measured from RS and (**a**) SWNT-1-CNTS, (**b**) SWNT-2-CNTS or (**c**) GS. To calculate toughness values, a mean silk density value of 1.34 g/cm^3 is used.

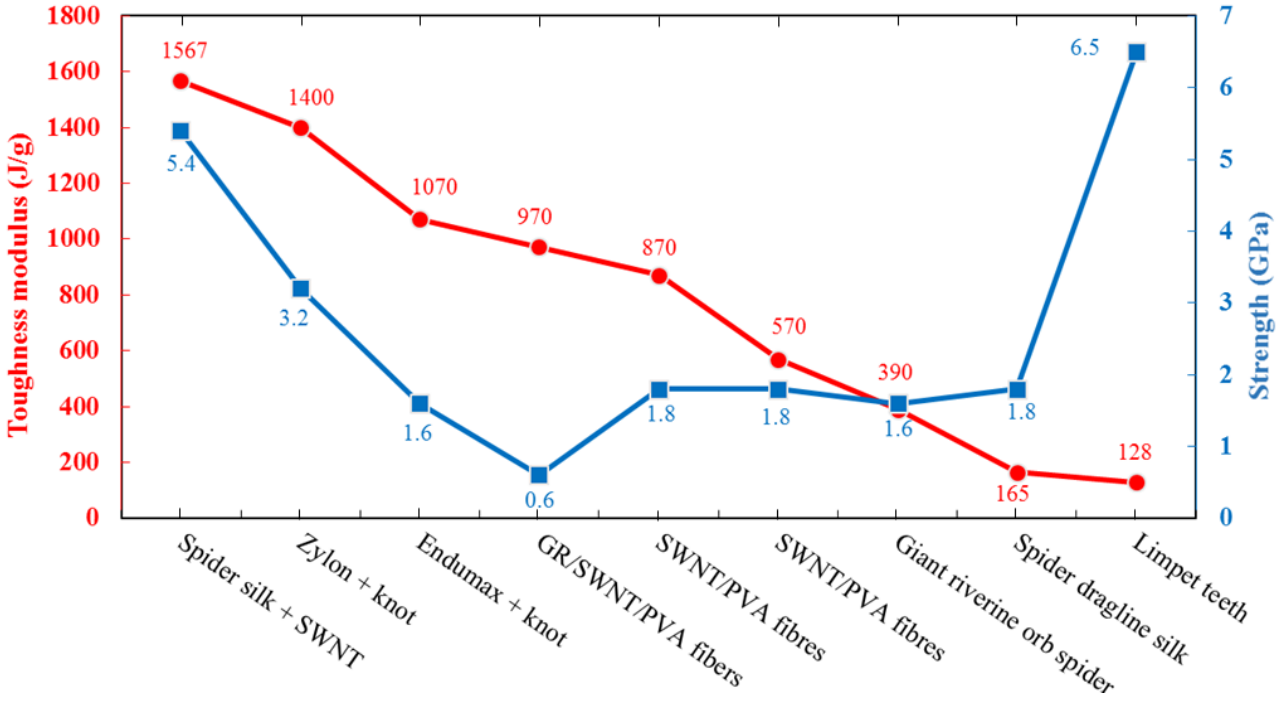

Figure 5: Toughness modulus and strength of different materials and composites.

TABLES

Table 1. Mechanical properties (average values) of RS samples.

Spider n.	Diameter (μm)	Number of threads	Young's Modulus (GPa)	Ultimate Strain (mm/mm)	Fracture Strength (MPa)	Toughness Modulus (MPa)
1	0.51±0.10	15	6.0±3.6	0.29±0.12	795.2±500.1	128.2±97.2
2	0.72±0.15	7	27.3±5.0	0.58±0.23	2397.2±635.5	713.0±138.5
3	0.75±0.11	10	13.4±6.9	0.46±0.40	1257.5±1299.3	422.6±567.6
4	0.69±0.06	108	1.9±0.6	1.38±1.11	465.1±119.0	235.6±126.2
5	0.71±0.06	128	3.2±0.8	1.02±0.30	534.7±222.1	172.4±77.4
6	0.72±0.02	2	37.1±19.6	0.28±0.06	4045.9±1391.6	732.1±354.9
7	0.86±0.07	10	15.1±6.4	0.39±0.07	1726.6±565.3	476.4±257.8
8	0.65±0.05	113	2.1±2.0	0.69±0.40	179.7±164.0	61.1±79.3
9	0.51±0.04	95	5.9±5.0	0.53±0.44	580.7±482.9	205.3±179.8
10	0.81±0.09	48	3.0±1.5	0.55±0.08	281.2±179.6	75.3±45.8
11	0.51±0.05	111	24.3±13.5	0.75±0.29	1969.1±1158.8	764.7±640.5
12	0.83±0.06	17	3.1±0.1	0.77±0.10	173.4±0.1	48.9±0.1
13	0.66±0.06	74	5.5±5.0	0.88±0.74	648.6±501.9	320.3±385.8
14	1.02±0.03	64	3.8±1.1	1.71±0.87	364.0±164.1	247.8±111.2
15	0.54±0.02	4	9.2±1.5	0.26±0.06	825.2±182.9	101.8±9.6

Table 2. Mechanical properties (average values) of the first collection of silk samples produced after exposure of the spiders to CNTs or graphene (Spiders n. 1-6 with SWNT-1, spiders n. 7-10 with SWNT-2, spiders n. 11-15 with graphene). The largest increments in the silk mechanical properties are observed for spider 5 whereas the highest absolute values are observed for spider 7.

Spider n.	Diameter (μm)	Number of threads	Reinforcement	Young's Modulus (GPa)	Ultimate Strain (mm/mm)	Fracture Strength (MPa)	Toughness Modulus (MPa)
1	0.57±0.04	27	SWNT-1	3.9±3.9	0.62±0.65	326.1±150.6	66.7±60.9
2	0.43±0.02	4	SWNT-1	40.1±48.4	0.20±0.16	3914.6±5038.3	587.2±820.3
3	0.77±0.09	72	SWNT-1	8.7±6.9	0.68±0.37	1195.8±1037.5	387.0±384.7
4	0.76±0.07	44	SWNT-1	2.4±0.6	0.95±0.52	579.4±313.1	187.6±66.7
5	0.78±0.08	4	SWNT-1	37.9±4.4	0.60±0.28	3907.2±874.1	1144.0±555.3
6	0.84±0.068	12	SWNT-1	9.6±5.2	0.50±0.24	954.3±278.2	210.2±87.3
7	1.00±0.12	62	SWNT-2	47.8±18.0	0.75±0.09	5393.5±1202.4	2143.6±684.6
8	0.42±0.08	34	SWNT-2	3.1±1.1	0.41±0.11	315.7±124.7	47.8±22.8
9	0.42±0.04	82	SWNT-2	19.3±6.3	0.34±0.14	2034.9±212.8	419.8±96.2
10	0.81±0.09	48	SWNT-2	0.2±0.0	0.32±0.02	20.1±3.5	2.6±1.8
11	0.67±0.02	43	GS	0.8±0.6	0.33±0.19	58.0±22.9	7.9±3.4
12	0.74±0.13	41	GS	4.9±1.1	0.43±0.06	607.5±219.2	148.5±71.6
13	0.66±0.06	74	GS	3.1±1.7	0.52±0.37	421.8±251.3	130.3±129.0
14	1.02±0.03	64	GS	0.4±0.2	0.29±0.08	45.9±17.1	6.0±2.8
15	0.61±0.06	14	GS	13.0±6.5	0.43±0.24	1245.6±559.4	254.7±164.3